The 2nd Joint International Conference on Multibody System Dynamics
May 29–June 1, 2012, Stuttgart, Germany

Development of a Wear Model for the Wheel Profile Optimization in the Railway Field

M. Ignesti*, A. Innocenti*, L. Marini*, E. Meli*, A. Rindi*, P. Toni*

* Department of Energy Engineering
University of Florence
Via S. Marta n. 3, 50139 Firenze, Italy
[ignesti, innocenti, marini, meli, rindi]@mapp1.de.unifi.it

1 Abstract

The prediction and the reduction of wear due to wheel-rail interaction is a fundamental aspect in the railway field, mainly correlated to stability and safety conditions and to maintenance interventions and costs.In this work the Authors present two innovative wheel profiles, specifically designed with the aim of improving the wear behaviour of the standard ORE S1002 wheel profile matched with the UIC 60 rail profile canted at 1/20 rad, which represents the wheel-rail combination occurring in Italian railway line. These two wheel profiles, conventionally named CD1 wheel profile and DR2 wheel profile, have been developed by the Authors in collaboration with Trenitalia S.p.A.. The CD1 wheel profile has been designed with the purpose of distributing the contact points in the flange zone on a larger area in order to reduce wear phenomena and having a costant equivalent conicity value in a band around the nominal contact point (when the generical wheelset is not shifted from the central position). The DR2 wheel profile is instead designed in order to keep the kinematic characteristics of the matching formed by ORE S1002 wheel profile and UIC 60 rail profile with laying angle α_p equal to 1/40 rad, widely common in European railways and characterised by good performances in both wear and kinematic behaviour.

2 Introduction

Wheel/rail interaction represents a critical aspect in railway applications since the evolution of rail and wheel profiles due to wear involves serious effects on both dynamics and stability of vehicles. A reliable wear model can also be used to optimize the original profiles and to obtain a more uniform wear on rolling surfaces in order to reduce the overall amount of worn material. The optimum combination of wheel and rail profiles is usually pursued through the design of a new wheel profile which matches an existing rail profile, because the cost of rail interventions is notably higher compared with the cost of interventions on the wheels. This paper describes the wear behaviour of two innovative wheel profiles, designed by the Authors in collaboration with Trenitalia and RFI, with the aim of reducing wheel/rail wear occuring when ORE S 1002 wheel profile and UIC 60 rail profile with laying angle α_p equal to 1/20 rad are coupled, as it occurs in Italian lines. The two new profiles are conventionally named CD1 wheel profile and DR2 wheel profile [6]. Wear profiles evolution has been estimated by means of a model specifically developed and validated by the Authors in previous works [5]: this model consists in two interactive parts: the *vehicle model* (formed by the multibody model and the 3D global contact model) and the *wear model* (which comprises the local contact model, the wear estimation and the profiles updating). The multibody model represents the dynamics of the vehicle to be studied and it is implemented in the Simpack Rail environment, while the 3D global contact model detects the wheel/rail contact points through an innovative algorithm based on suitable semy-analytical procedures and then, for each contact point, calculates the contact forces by means of Hertz and Kalker's theory [4]. Thanks to the numerical efficiency of the new contact model, it can interact directly online with the multibody model during the dynamic simulation of the vehicle. Profiles evolution due to wear is then evaluated by means of a local contact model (in this case the Kalker's FASTSIM algorithm) and through an experimental relationship for the calculation of the worn material available in literature [2]. To evaluate the capability in wear reduction of the two innovative profiles, the passenger vehicle ALSTOM *Aln 501 Minuetto* has been modeled. All the simulations are performed on a virtual track, designed to represent a statistical description of the whole Italian railway line [6]. The data necessary to build the multibody model of the vehicle and the virtual track model were respectively provided by Trenitalia S.p.A and RFI [6].

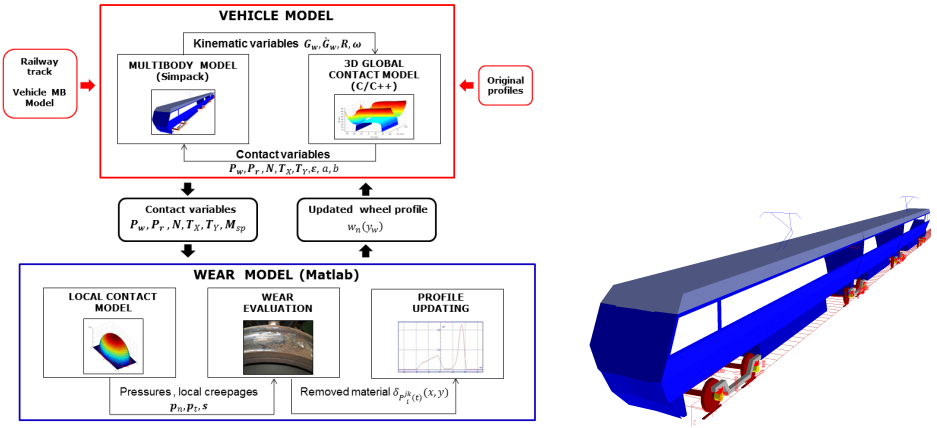

(a) General architecture of the model.

(b) Global view of the multibody model.

Figure 1. General architecture and multibody model.

3 General Architecture of the Model

The general architecture of the model consists in a procedure articulated in two separate parts that work alternatively at each procedure step: the *vehicle model* and the *wear model*. The general layout of the entire model is shown in Figure 1a. The *vehicle model* is the part responsible for the dynamical simulations, performed through the online mutual interaction of two sub-models, the multibody model of the investigated vehicle (in this work the ALSTOM *Aln 501 Minuetto*) and the 3D global contact model. At each integration step during time-domain dynamic simulation, the multibody model computes the kinematic variables (position, orientation and their derivatives) of the considered vehicle at each wheelset. These variables are then passed to the 3D global contact model, which calculates the global contact parameters: contact points, contact areas, global creepages and contact forces. In particular, the contact points detection is based on an innovative algorithm developed by the Authors in previous works [5], while the contact forces (normal and tangential forces) are evaluated through Hertz and Kalker's global theories [4]. Once the tangential contact problem has been solved, the values of the global forces are sent back to the multibody model and the dynamical simulation proceeds with the next time integration step. The *wear model* predicts the amount of worn material to be removed from the wheel surfaces. It can be sub-divided into three parts: the local contact model, the evaluation of worn material and the profile updating. Firstly, the local contact model (Hertz's local theory and Kalker's simplified theory implemented in FASTSIM algorithm) estimates the local contact pressures and creepages and detects the creep zone of the contact area. Then, according to an experimental relationship between the worn material and the energy dissipated by friction forces at the contact interface available in literature [2], the quantity of removed material on wheel surface is computed on the creep area. This is performed hypothesizing dry contact friction at the wheel/rail interface as Trenitalia and RFI requirements estabilish. Last step of the wear prediction procedure consists in updating the profiles: the worn profiles are derived from the original ones using an appropriate update strategy. The resulting new profiles are then fed back as input to the *vehicle model* and the whole model procedure proceeds with the next discrete step. In the present work the total mileage km_{tot} is subdivided in steps characterized by a variable adaptive lenght km_{step} and the wheel profile is supposed to be costant within each discrete step (corresponding to a traveled distance equal to km_{step}). It is worth noticing that a decrease of the km_{step} value increases the model precision and, at the same time, the computational effort. The adopted updating strategy may appreciably affects the results and its main task consists in choosing the appropriate discrete steps for the update of wheel profiles. Two different strategies are available in literature; these strategies are: the constant step update strategy, which is characterized by a constant value km_{step} of the discrete step and the adaptive step update strategy, wherein the profile is updated when a given threshold of the maximum value of cumulative wear depth is reached (the value km_{step} is consequently variable). During this research activity the adaptive step has been adopted for its capacity in representing the non-linear wear evolution (particularly in the first phase of the simulations, characterized by non conforme wheel/rail contact). Furthermore, this strategy presents computational times comparable with those relative to the constant step update strategy.

4 The Vehicle Model

The present section introduces the *vehicle model*, which consists in the multibody model of the studied vehicle and in the algorithm that models the 3D global contact.

The trainset to be investigated is ALSTOM *Aln 501 Minuetto* [6], a passenger transport unit widespread in Italian Railways. The multibody model (Figure 1b) of the vehicle has been implemented in the Simpack multibody environment and it is totally made up by thirty-one rigid bodies: three coaches, four bogies (two external motor bogies and two intermediate trailer bogies interposed between two successive coaches), eight wheelsets and sixteen axleboxes.The dual-stage suspensions have been modeled by means of three-dimensional linear and non linear visco-elastic force elements. In the primary suspension stage the elastic elements are Flexicoil springs while damping of the vertical relative displacement is given by two non linear dampers. The secondary stage is formed by pneumatic suspensions and it comprises the following elements: two air springs, six non linear dampers (lateral, vertical and anti-yaw dampers), one non linear traction rod, the roll bar, two non linear lateral bumpstops.

In the present research a specifically developed 3D global contact model has been used to improve reliability and accuracy of the contact points detection, compared to those given by the Simpack Rail contact model. The adopted contact model is based on a two step procedure; at the first step the contact points number and positions are determined through an innovative algorithm, namely the Distance Method, designed and validated by the Authors [5]. During the second step, for each detected contact point, the global contact forces are evaluated with Hertz and Kalker's global theories [4].

5 The Wear Model

The current section describes the three phases constituting the wear model: the local contact model, the computation of the amount of worn material (assuming dry contact conditions) and the wheel profile update.

The wear model inputs are the global contact parameters estimated by the vehicle model. Since a local wear computation is required, the global contact parameters need to be post-processed by a local contact model and this can be achieved with the simplified Kalker's theory implemented in the FASTSIM algorithm. This theory starts from the global creepages (ε), the normal and tangential global forces (N^r, T_x^r, T_y^r), the contact patch dimensions (a, b) and the material properties to compute the local distribution of normal p_n and tangential $\mathbf{p}_t$ stresses and local creepages $\mathbf{s}$ across the wheel/rail contact area. For a more detailed description of the FASTSIM algorithm one can refers to the literature [4].

The distribution of worn material on wheel profile is evaluated by means of a wear experimental function, based on a relation between the energy dissipated in the wheel-rail contact patch and the amount of worn material [2]. The adopted wear function uses normal p_n and tangential $\mathbf{p}_t$ stresses, creepages $\mathbf{s}$ and the vehicle velocity V as the input to compute directly the specific volume of worn material $\delta_{P_{wi}^{jk}(t)}(x,y)$ ($mm^3/(m \cdot mm^2)$) related to the i-th contact point $P_{wi}^{jk}(t)$ on the j-th wheel relative to the k-th dynamical simulation (for unit of distance traveled by the vehicle (expressed in m) and for unit of surface (expressed in mm^2)). More specifically, local stresses and creepages are used to evaluate the *wear index* I_W (expressed in N/mm^2), which represents the frictional power developed by the tangential contact pressures: $I_W = \frac{\mathbf{p}_t \bullet \mathbf{s}}{V}$. This index can be correlated with the *wear rate* K_W which represents the mass of removed material (expressed in $\mu g/(m \cdot mm^2)$) for unit of distance traveled by the vehicle and for unit of surface. The correlation is based on real data available in literature [2], derived from experimental wear tests carried out in the case of metal to metal contact with dry surfaces using a twin disc test arrangement. The experimental relationship between K_W and I_W chosen for the development of the present wear model is described by the following equation:

$$K_W(I_W) = \begin{cases} 5.3 * I_W & I_W < 10.4 \\ 55.12 & 10.4 \leq I_W \leq 77.2 \\ 61.9 * I_W - 4778.68 & I_W > 77.2. \end{cases} \quad (1)$$

Once the wear rate $K_W(I_W)$ has been computed, the corresponding specific volume of worn material (for unit of distance traveled by the vehicle and for unit of surface) can be calculated as follows (expressed in $mm^3/(m \cdot mm^2)$): $\delta_{P_{wi}^{jk}(t)}(x,y) = K_W(I_W)\frac{1}{\rho}$ where ρ is the material density (expressed in kg/m^3).

After obtaining the amount of worn material, wheel profile needs to be updated to get the new profile, denoted by $w_n(y_w)$, which is computed from the old one $w_o(y_w)$ and from all the calculated distributions of worn material $\delta_{P_{wi}^{jk}(t)}(x,y)$ through an appropriate numerical procedure that defines the update strategy. The update strategy is also applied to reduce the numerical noise characterising the distribution $\delta_{P_{wi}^{jk}(t)}(x,y)$ that can generates problems to the global contact model. Another issue to be provided from the update procedure is the average of the worn material distributions. In fact, according to Trenitalia and RFI requirements, the output of the wear model must be a single profile; hence the evaluated distribution $\delta_{P_{wi}^{jk}(t)}(x,y)$ needs to be mediate. The whole numerical procedures which computes the new profiles is formed by a set of succeeding integrations:

1) *Longitudinal integration* which provides the mean value of wheel worn material expressed in $mm^3/(m \cdot mm^2)$ by summing in the longitudinal direction all the wheel wear contributions inside the contact path and distributing the resulting quantity along the wheel circumference of lenght $2\pi w(y_{wi}^{jk})$:
$\frac{1}{2\pi w(y_{wi}^{jk})} \int_{-a(y)}^{+a(y)} \delta_{P_{wi}^{jk}(t)}(x,y)dx = \delta_{P_{wi}^{jk}(t)}^{tot}(y)$.
2) *Time integration*: $\int_{T_{ini}}^{T_{fin}} \delta_{P_{wi}^{jk}(t)}^{tot}(y)V(t)dt \approx \int_{T_{in}}^{T_{end}} \delta_{P_{wi}^{jk}(t)}^{tot}(s_w - s_{wi}^{cjk}(t))V(t)dt = \Delta_{P_{wi}^{jk}}(s_w)$ where the natural abscissa s_w relative to the curve $w(y_w)$ has been introduced. The following relations locally hold: $y \approx s_w - s_{wi}^{cjk}(t)$ and $w(y_w) = w(y_w(s_w)) = \tilde{w}(s_w)$.The natural abscissa of the contact point s_{wi}^{cjk} can be evaluated starting from its position P_{wi}^{jk}. Therefore the longitudinal integration sums all the wear contributions relative to the dynamic simulation and gives as output the depth of worn material due to the considered contact point $\Delta_{P_{wi}^{jk}}(s_w)$ in $mm = mm^3/mm^2$.
3) *Sum on the contact points*: $\sum_{i=1}^{N_{PDC}} \Delta_{P_{wi}^{jk}}(s_w) = \Delta_{jk}^{w}(s_w)$ where N_{PDC} represents the maximum number of contact points that can be considered for each single wheel. The output $\Delta_{jk}^{w}(s_w)$ is the removed material of the j-th wheel during the k-th simulation. The number of active contact points changes during the simulation but it is usually less than N_{PDC}; thus, the amount of worn material due to non-active contact points is automatically set equal to zero.
4) *Average on the vehicle wheels and on the dynamic simulations*: $\sum_{k=1}^{N_c} p_k \frac{1}{N_w} \sum_{j=1}^{N_w} \Delta_{jk}^{w}(s_w) = \overline{\Delta}^{w}(s_w)$ where N_w is the number of vehicle wheels while the p_k, $1 \leq k \leq N_c$, $\sum_{k=1}^{N_C} p_k = 1$ are the statistical coefficients related to the various dynamic simulations, estabilished by the statistical analysis as will be better explained in the following sections. The average on the number of wheel-rail interactions has to be performed to obtain as output of the wear model a single average profile for the wheel (as required by Trenitalia and RFI).
5) *Scaling*: Since it normally takes traveled distance of thousands kilometers in order to obtain measurable effects of wheel wear, an appropriate scaling procedure is necessary to reduce the simulated track lenght with a consequent limitation of the computational effort. The total mileage km_{tot} traveled by the vehicle is chosen according to the purpose of the simulations, for example equal to the re-profiling intervals. This mileage is subdivided in steps characterized by a lenght equal to km_{step} and the wheel profile is supposed to be costant within each discrete step (corresponding to a traveled distance equal to km_{step}). The km_{step} value represents a distance which is still too long to be simulated in reasonable computational times. However this can be overcome as follows: a linear relationship between the amount of worn material and the traveled distance is supposed to hold only inside the discrete step; according to this hypothesis a notably smaller distance km_{prove} can be simulated and the relative amount of wheel worn material can be amplified in order to evaluate the worn material distribution relative to the km_{step} traveled distance.
The discrete step definition can be done according to the following two main update strategies: the constant step update strategy (characterized by a constant value km_{step} of the discrete step) and the adaptive step update strategy wherein the profile is updated when a given threshold Δ_{fix} on the maximum value $\Delta_{max} = \max_{s_w} \overline{\Delta}(s_w)$ of cumulative wear depth is reached (the value km_{step} is consequently variable). In the present research the adaptive step approach has been chosen and the discrete step value km_{step} can be defined through the following equation: $km_{step} = km_{prove} \frac{\Delta_{fix}}{\Delta_{max}}$ where $km_{prove} = l_{track}$ is the traveled distance simulated during the N_c dynamic analysis. The quantity Δ_{max} represents the maximum cumulative wear depth while Δ_{fix} is the related chosen threshold value and in this work it is equal to $0.1\ mm$. The scaled amount $\overline{\Delta}^{sc}(s_w)$ of worn material to be removed by the wheel surface is then given by the following expression: $\overline{\Delta}^{sc}(s_w) = \overline{\Delta}(s_w) \frac{\Delta_{fix}}{\Delta_{max}}$.
6) *Smoothing of the worn material*: $\Im\left[\overline{\Delta}^{wsc}(s_w)\right] = \overline{\Delta}_{sm}^{wsc}(s_w)$; the numerical noise and short wave-

lenghts without physical meanings that affect the worn material distribution can be passed to the new wheel profile $\tilde{w}_n(s_w)$ with consequent problems raising in the global contact model. Hence an appropriate smoothing of the worn material distributions is required and this is achieved by means of a first-order discrete filter (moving average).

7) *Profile update:* $\begin{pmatrix} y_w(s_w) \\ \tilde{w}_o(s_w) \end{pmatrix} - \overline{\Delta}^{wsc}_{sm}(s_w)\mathbf{n}^r_w \xrightarrow{re-parameterization} \begin{pmatrix} y_w(s_w) \\ \tilde{w}_n(s_w) \end{pmatrix}$; the last step of the procedure consists in the determination of the new wheel profile $\tilde{w}_n\big(s\big) = w_n\big(y\big)$ starting from the old one $\tilde{w}_o\big(s\big) = w_o\big(y\big)$.

6 Setting-up of the Minuetto Virtual Track

When the wear analyses have to be carried out on a set of tracks of considerable length by using at the same time accurate models for the vehicle and the wheel-rail contact, the utilisation of "railway line statistical model" may be a indispensable way to overcome a series of problems due to the computational times and the organisation of the simulations themselves. The basic idea is to substitute a complex railway net or the too long tracks to be simulated with a set of simpler tracks which can produce an equivalent amount and distribution of wear on wheels. In such cases it is fundamental to sum up in a statistical model of the whole railway net the most relevant information about the real context on which the vehicles operate, in order to get results in terms of average behaviour of the vehicle-wheel profile matching considered. In the present work the statistical approach has been exploited to draw up the mean line of the Minuetto train. This mean line had to be a significant and equivalent synthesis of the whole set of tracks in Italian railways on which the train composition operate every day. The same strategy has also been used in drawing up a virtual track of the Aosta-Pre Saint Didier line aimed at the model validation via comparison with the available experimental results described in [3]. The application of the statistical methodology has provided the mean line reported in Tab. 1, made up of 34 classes: for each track, the mean radius, the speed, the superelevation and the statistical weight of each class have been specified.

Table 1. The Minuetto virtual track.

R_{min} (m)	R_{max} (m)	R_m (m)	Δh (mm)	h (mm)	V (km/h)	p_k %
250	278	**263**	90–120	90	65	1.90
			130–160	160	75	4.21
278	313	**294**	90–120	90	70	1.11
			130–160	160	80	1.62
313	357	**333**	90–120	90	70	0.44
			130–160	140	80	1.24
357	417	**385**	50–80	50	70	0.80
			90–120	120	80	1.33
			130–160	150	90	4.17
417	500	**455**	50–80	80	70	1.44
			90–120	100	80	4.72
			130–160	130	90	1.29
500	625	**556**	10–40	10	70	0.14
			50–80	80	80	1.52
			90–120	90	85	2.01
			130–160	150	110	1.46
625	833	**714**	10–40	10	70	0.09
			50–80	70	85	1.56
			90–120	90	95	1.77
			130–160	130	115	0.78
833	1250	**1000**	10–40	10	70	1.10
			50–80	50	85	2.41
			90–120	120	130	2.16
			130–160	140	140	0.93
1250	2500	**1667**	0	0	70	0.17
			10–40	30	85	1.91
			50–80	80	140	1.68
			90–120	90	145	0.99
			130–160	150	160	0.17
2500	10000	**5000**	0	0	70	1.08
			10–40	20	120	1.21
			50–80	50	160	0.25
			90–120	100	160	0.004
		∞				52.3

In this work, the available data on the rail profiles provided by RFI have been exploited to select a series of rail profiles to be used as time-independent profiles in the multibody simulations. According to the working hypothesis that in small radius curves it is easier to find a deeply worn rail profile than in straight tracks or

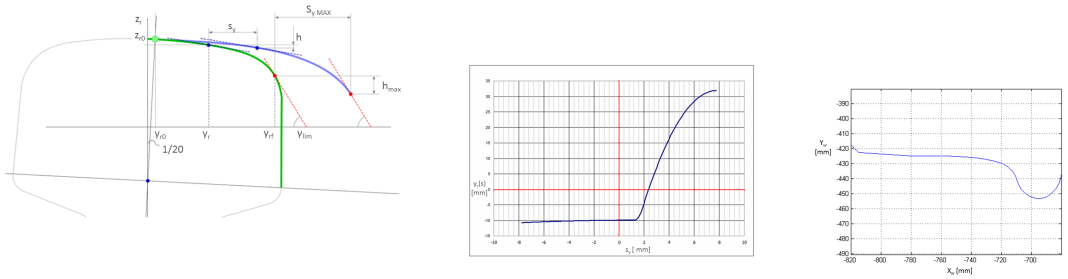

(a) Design procedure of the CD1 wheel profile.

(b) Graphical representation of the definitive $y_r(s_y)$.

(c) CD1 wheel profile.

Figure 2. The CD1 wheel profile.

in large radius curves, a pair of representative (in statistical sense) worn rail profiles has been chosen for each radius curve range.

7 Description of the proposed wheel profiles

This section describes the procedures for the design of the two proposed wheel profiles, named CD1 and DR2 wheel profile. These procedures have been developed by the Authors in collaboration with Trenitalia and RFI [6].

The CD1 wheel profile has been designed in order to achieve the two following goals: increase of the contact area in the flange zone in order to improve wear characteristics thanks to a better distribution of the contact points and mantaining the target constant value of the equivalent conicity in a band around the nominal contact point (when the wheelset is in the neutral position). The adopted nomenclature for the wheel profile construction is shown in Figure 2a. The abscissa y_w characterising the points of the new wheel profile are calculated starting from the abscissa y_r of the rail profile (with $y_{r0} \leq y_r \leq y_{rf}$) according to the expression:

$$y_w = y_r(s_y) + s_y \tag{2}$$

where s_y is the variable representing the horizontal gap between wheel and rail profile; its value can vary from 0 to the maximum desired horizontal gap s_{yMAX}. The relationship $y_r(s)$, occurring between the two horizontal variables can be chosen arbitrarly; once the relation has been defined, for each value y_r of the rail profile the corresponding value of s_y can be obtained. According to the purpouses previously described, it has been adopted the relationship illustrated in the graphical representation of Figure 2b. The z_w value can be evaluated from the corresponding rail value z_r:

$$z_w = z_r(y_r(s_y)) - h(s_y) \quad h(s_y) = -\int_0^{s_y} tan\left(\gamma(y_r(s'_y))\right) ds'_y. \tag{3}$$

The variable $\gamma(y_r(s'_y))$ represents the contact angle formed by the tangent to the rail profile point identified by $y_r(s')$ value and the horizontal plane. The resulting CD1 wheel profile is illustrated in Figure 2c.

The design of the DR2 wheel profile aims to guarantee the kinematic characteristics of the original matching formed by ORE S1002 wheel profile and UIC 60 rail profile with laying angle α_p equal to 1/40 rad, also with the new matching DR2 wheel profile - UIC 60 rail profile canted at 1/20 rad. The original matching has been chosen because it is widely common in European railways and it is characterised by good performances in both wear and kinematic behaviour. The nomenclature adopted for the profile construction is shown in Figure 3 where the apexes r and w respectively refer to auxiliary and local reference system while the apexes 1 and 2 denote the right and left wheel. The position of the local reference system origin expressed in the auxiliary reference system is denoted by: $\mathbf{O}_w^r = [\ y \quad z(y)\ ]^T$.
In the present research activity, the purpouse in mantaining the kinematic properties of the ORE S 1002 - UIC 60 canted at 1/40 rad matching is achieved by supposing that some variables of the new matching (DR2 wheel profile - UIC 60 matching canted at 1/20 rad) remain the same of the original ones (in the remaining of the article the variables characterising the original matching and those referring to the new

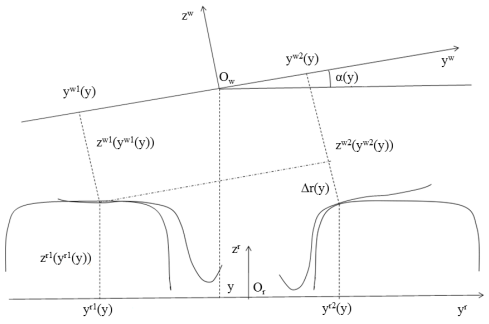

Figure 3. Adopted nomenclature for DR2 design.

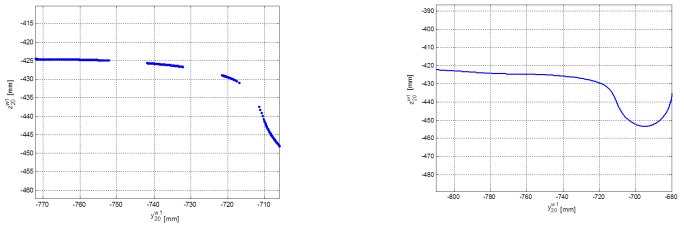

(a) (b)

Figure 4. Distribution of contact points after applying the design procedure (a), the DR1 wheel profile (b).

matching will be respectively denoted with the subscripts 40 and 20). More specifically the design procedure requires six inputs from the old matching $y_{40}^{r1}(y)$, $y_{40}^{r2}(y)$, $\alpha_{40}(y)$, z_{40}^{r}, $z_{40}^{r1}(\bullet)$,$z_{40}^{r2}(\bullet)$ and two inputs from the new matching $z_{20}^{r1}(\bullet)$,$z_{20}^{r2}(\bullet)$. Then, starting from these inputs, the equations describing the coordinate transformation of the contact points between the local and the auxiliary reference system can be written both for the original matching:

$$\begin{pmatrix} y_{40}^{r1} \\ z_{40}^{r1}(y_{40}^{r1}) \end{pmatrix} = \begin{pmatrix} y \\ z_{40} \end{pmatrix} + R(\alpha_{40}) \begin{pmatrix} y_{40}^{w1} \\ z_{40}^{w1}(y_{40}^{w1}) \end{pmatrix}, \quad \begin{pmatrix} y_{40}^{r2} \\ z_{40}^{r2}(y_{40}^{r2}) \end{pmatrix} = \begin{pmatrix} y \\ z_{40} \end{pmatrix} + R(\alpha_{40}) \begin{pmatrix} y_{40}^{w2} \\ z_{40}^{w2}(y_{40}^{w2}) \end{pmatrix} \tag{4}$$

and for the new matching:

$$\begin{pmatrix} y_{40}^{r1} \\ z_{20}^{r1}(y_{40}^{r1}) \end{pmatrix} = \begin{pmatrix} y \\ z_{40} \end{pmatrix} + R(\alpha_{40}) \begin{pmatrix} y_{20}^{w1} \\ z_{20}^{w1}(y_{20}^{w1}) \end{pmatrix}, \quad \begin{pmatrix} y_{40}^{r2} \\ z_{20}^{r2}(y_{40}^{r2}) \end{pmatrix} = \begin{pmatrix} y \\ z_{40} \end{pmatrix} + R(\alpha_{40}) \begin{pmatrix} y_{20}^{w2} \\ z_{20}^{w2}(y_{20}^{w2}) \end{pmatrix} \tag{5}$$

where the wheelset lateral displacement value y is bounded in the range $[-y_M, y_M]$. The outputs of the design procedure that characterise the new wheel profile are the lateral $y_{20}^{w1}(y)$, $y_{20}^{w2}(y)$ and vertical $z_{20}^{w1}(y_{20}^{w1}(y))$, $z_{20}^{w2}(y_{20}^{w2}(y))$ coordinates of the contact points of the new wheel profile in the local reference system. The design procedure is performed in a discrete way for every y value of the discrete range. It should be noticed that the resulting profile is characterized by holes (see Figure 4), that are the regions where there isn't any computed contact point. In the present procedure these regions have been filled fitting the computed points with spline functions and the resulting wheel profile, named DR1, is illustrated in Figure 4b.

The geometrical wheel/rail contact characteristics are ruled by the rolling radii difference, that is the difference between rolling radii of the right and the left wheels for each lateral displacement y and it is defined with the following expressions respectively valid for the original (ORE S1002 wheel profile and UIC 60 canted at 1/40) and the resulting matching: $\Delta r_{40} = z_{40}^{w2}(y_{40}^{w2}(y)) - z_{40}^{w1}(y_{40}^{w1}(y))$, $\Delta r_{20} = z_{20}^{w2}(y_{20}^{w2}(y)) - z_{20}^{w1}(y_{20}^{w1}(y))$. The adopted design procedure implies that the rolling radii difference Figure

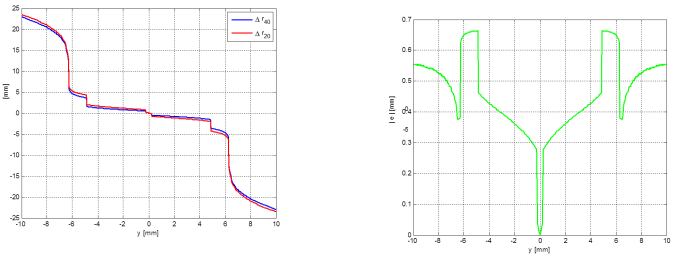

(a) (b)

Figure 5. DR1-UIC 60 canted at 1/20 matching: rolling radius difference (a), error in rolling radii difference (b).

5a of the new matching is equal to the one characterizing the original matching, disregarding a small estimable variation $e = \Delta r_{20} - \Delta r_{40}$ (see Figure 5b). Subtracting from each other the equations (4) and the equations (5), it leads to the following expressions:

$$\begin{pmatrix} y_{40}^{r2} - y_{40}^{r1} \\ z_{40}^{r2}(y_{40}^{r2}) - z_{40}^{r1}(y_{40}^{r1}) \end{pmatrix} = R(\alpha_{40}) \begin{pmatrix} y_{40}^{w2} - y_{40}^{w1} \\ \Delta r_{40} \end{pmatrix}, \quad \begin{pmatrix} y_{40}^{r2} - y_{40}^{r1} \\ z_{20}^{r2}(y_{40}^{r2}) - z_{20}^{r1}(y_{40}^{r1}) \end{pmatrix} = R(\alpha_{40}) \begin{pmatrix} y_{20}^{w2} - y_{20}^{w1} \\ \Delta r_{20} \end{pmatrix} \tag{6}$$

Then, subtracting on turn the equations (6) it holds: $R_{(\alpha_{40})}^{T} \begin{pmatrix} 0 \\ \Delta z_{20}^{r} - \Delta z_{40}^{r} \end{pmatrix} = \begin{pmatrix} \Delta y_{20}^{r} - \Delta y_{40}^{r} \\ \Delta r_{20} - \Delta r_{40} \end{pmatrix}$. The second component of the previous equation leads to an expression of the rolling radii functions variation between the new and the original matching:

$$(\Delta z_{20}^{r} - \Delta z_{40}^{r}) \cos \alpha_{20} = \Delta r_{20} - \Delta r_{40} = e(y) \tag{7}$$

which is function of the wheelset lateral displacement. In order to improve the rolling radii difference error between the original matching and DR1 wheel profile - UIC 60 canted at 1/20 matching, an optimization algorithm has been developed. The basic idea of this algorithm consists in translating the lateral input coordinates $y_{40}^{r1}(y)$,$y_{40}^{r2}(y)$ of a certain quantity $k(y)$, evaluated through a minimization process of the rolling radii error for each possible lateral wheelset displacement y. The lateral coordinates of the contact points in the auxiliary reference system can be then re-defined as: ${y_{40}^{r1}}^{k} = y_{40}^{r1} + k$, ${y_{40}^{r2}}^{k} = y_{40}^{r2} + k$ where the k value is bounded in the range $[-\bar{k}, +\bar{k}] = I_k$. Therefore the expression of the rolling radii error becomes a function of both y and k value:

$$E(y,k) = \cos \alpha_{20}(z_{20}^{r2}(y_{40}^{r2} + k) - z_{20}^{r1}(y_{40}^{r1} + k) - z_{40}^{r2}(y_{40}^{r2}) + z_{40}^{r1}(y_{40}^{r1})). \tag{8}$$

Equation 8 is used as the objective function to find the optimal value k_{opt} of the translation quantity, which is defined for each wheelset lateral displacement y. The optimization process has been performed in a discrete way: $k_{opt}(y) = \arg\min_{k \in I_k} |E(y,k)|$. The resulting lateral coordinates of the contact points in the auxiliary reference system are evaluated as: $y_{opt}^{r1} = y_{40}^{r1} + k_{opt}$, $y_{opt}^{r2} = y_{40}^{r2} + k_{opt}$. Through introducing these coordinates into equations (5), the outputs $y_{20}^{w1}(y)$, $z_{20}^{w1}(y_{20}^{w1}(y))$, $y_{20}^{w2}(y)$, $z_{20}^{w2}(y_{20}^{w2}(y))$ of the optimized wheel profile UIC 60 rail canted at 1/20 matching are obtained according to the following expressions:

$$\begin{pmatrix} y_{opt}^{r1} \\ z_{20}^{r1}(y_{opt}^{r1}) \end{pmatrix} = \begin{pmatrix} y \\ z_{40} \end{pmatrix} + R(\alpha_{40}) \begin{pmatrix} y_{20}^{w1} \\ z_{20}^{w1}(y_{20}^{w1}) \end{pmatrix}, \quad \begin{pmatrix} y_{opt}^{r2} \\ z_{20}^{r2}(y_{opt}^{r2}) \end{pmatrix} = \begin{pmatrix} y \\ z_{40} \end{pmatrix} + R(\alpha_{40}) \begin{pmatrix} y_{20}^{w2} \\ z_{20}^{w2}(y_{20}^{w2}) \end{pmatrix}. \tag{9}$$

The optimized wheel profile, obtained after the holes fitting procedure and named DR2 wheel profile, is shown in Figure 6a. The new rolling radii difference function is compared with the original one in Figure 6b; it shows that the two plots are almost coincident and that the error (see Figure 6c), which depends on the discretization precision of the rangeI_k, is about zero. The design procedure adopted to define the DR2 discrete wheel profile may be affected by numerical errors coming from different sources like the use of splines in the holes and of fictitious points at the boundaries of the wheel profile (where there isn't a contact point distribution) and the subsequent resamplings and smooth process of profiles and their derivatives; moreover, since the DR2 wheel profile and UIC 60 rail canted at 1/20 matching is based on the geometrical

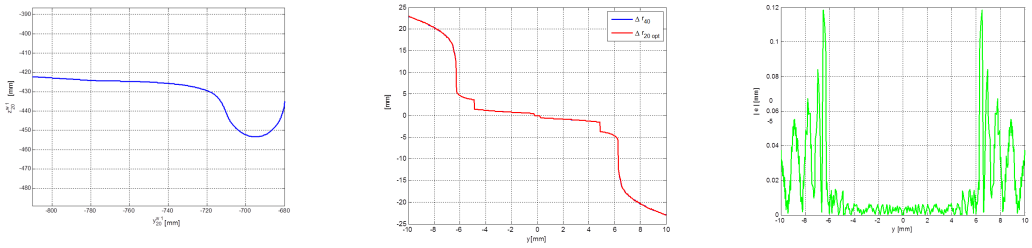

(a) The DR2 wheel profile. (b) Rolling radii difference distribution. (c) Error in rolling radii difference distribution

Figure 6. Characteristics of the DR2-UIC60 canted at 1/20 matching.

properties of the ORE S 1002-UIC 60 canted at 1/40 matching, the new matching is characterized by the stiffness caused by the conformal contact typical of the original one. At the same time, one of the numerical advantage of the procedure consists in the fact that the new DR2 wheel profile is designed without any condition on the derivatives of the profiles; this aspect involves a reduction of the smoothing requirements and doesn't further increase the ill-conditioning characteristic of the design problem.

8 Wear Analysis

In this section the results of the dynamic simulations aimed at a wear evaluation will be presented in order to compare the profiles considered in this study: the standard S1002 and the two innovative profiles (CD1, DR2). For what concerns the comparison in terms of resistance to wear, the performance can be assessed by analysing the evolution of three reference dimensions (qR quota, flange thickness fT and flange height fH, Fig. 7), according to the regulations in force [1], without a complete detection of the whole 2D profile. The Fig. 8a shows the progress of the mean qR dimension for each profile: as it can be seen, the progress

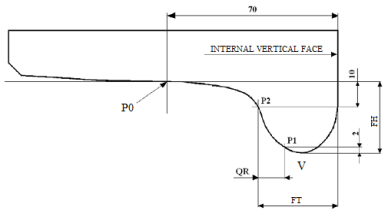

		$d \leq 630$	$630 < d \leq 760$	$760 < d$
fH	min	31.5	29.5	27.5
	max		36	
		$d \leq 760$	$760 < d \leq 840$	$840 < d$
fT	min	27.5	25	22
	max		33	
qR	min		6.5	

Figure 7. Reference dimensions of the wheel profile (left) and limit values in mm (right) for a wheel having an actual rolling diameter equal to d.

of the CD1 and DR2 profiles is slower than that of the S1002; in particular, the best performance is given by the DR2 profile. In fact, assuming a comparison limit equal to 7 mm, which is slightly above than the acceptable threshold value of 6.5 mm prescribed by the standard [1], the trend of the DR2 shows that the comparison limit is reached with an increase in the covered distance by at least 30%. In regarding to the progress of the flange thickness fT depicted in Fig. 8b, the minimum value equal to 22 mm [1] is reached after covering about 80 000 km when the S1002 profile is adopted on the Minuetto; differently, with the new profiles the total covered distance can be extend up to 100 000 km and above. Differently from the qR, in the reduction of the flange thickness the difference between the performance provided by the CD1 and DR2 profile is about 5% only. With respect to the evolution of the wheel shape, the comparison between the initial and the final condition for the three profiles is presented in Figg. 9a, 9b and 9c. The variation in wheel profile is numerically described by means of about one hundred procedure steps. Since the mean line of the Minuetto comprises a relevant percentage of sharp curves, the wear is mainly located on the flange instead of the tread.

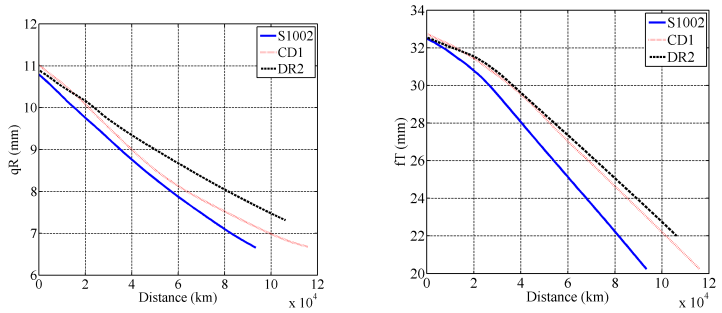

(a) (b)

Figure 8. Progress of the qR dimension (a) and the flange thickness fT (b): comparison of the three wheel profiles.

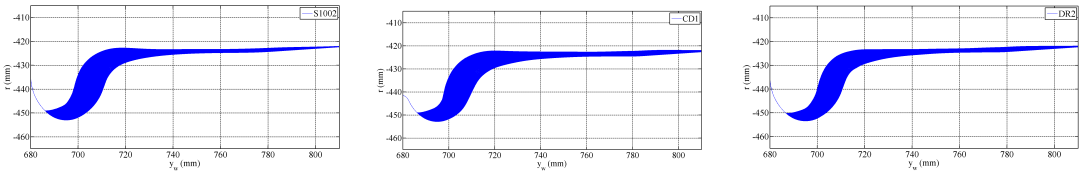

(a) S1002. (b) CD1. (c) DR2.

Figure 9. Wear progress on the three wheel profiles.

9 Conclusions

In this paper the author have presented a work focused on the development of a mathematical model for the wear evaluation in railway vehicles and on the comparison between the performance provided by different wheel profiles in terms of resistance to wear. More precisely, the standard ORE S1002 wheel profile widely used on vehicles in service on the Italian railways has been compared with two innovative wheel profiles developed by authors to improve the poor performance of the S1002 profile with regard to the resistance to wear and the guidance in sharp curves. The activity has been performed in collaboration with Trenitalia S.p.A and Rete Ferroviaria Italiana (the administrator of the Italian railway infrastructure) which provided the necessary technical and experimental data for the implementation of the whole procedure aimed at wear evaluation.

REFERENCES

[1] EN 15313: Railway applications — In-service wheelset operation requirements — In-service and off-vehicle wheelset maintenance, 2010.

[2] F. Braghin, R. Lewis, R. S. Dwyer-Joyce, and S. Bruni. A mathematical model to predict railway wheel profile evolution due to wear. *Wear*, 261:1253–1264, 2006.

[3] M. Ignesti, M. Malvezzi, L. Marini, E. Meli, and A. Rindi. Development of a wear model for the prediction of wheel and rail profile evolution in railway systems. *Wear*, 2012. DOI: 10.1016/j.wear.2012.01.020.

[4] J. J. Kalker. *Three-dimensional Elastic Bodies in Rolling Contact*. Kluwer Academic Publishers, Dordrecht, Netherlands, 1990.

[5] E. Meli, S. Falomi, M. Malvezzi, and A. Rindi. Determination of wheel - rail contact points with semianalytic methods. *Multibody System Dynamics*, 20:327–358, 2008.

[6] P. Toni. Ottimizzazione dei profili delle ruote su binario con posa 1/20. Technical report, Trenitalia S.p.A., 2010.